

Electric curing parameters of mortar and its mechanical properties in cold weather

ABUBAKRI, S., MANGAT, Pal <<http://orcid.org/0000-0003-1736-8891>>, STARINIERI, V. and LOMBOY, G.R.

Available from Sheffield Hallam University Research Archive (SHURA) at:

<https://shura.shu.ac.uk/29468/>

This document is the Accepted Version [AM]

Citation:

ABUBAKRI, S., MANGAT, Pal, STARINIERI, V. and LOMBOY, G.R. (2022). Electric curing parameters of mortar and its mechanical properties in cold weather. *Construction and Building Materials*, 314 (Part A). [Article]

Copyright and re-use policy

See <http://shura.shu.ac.uk/information.html>

1 **Abstract**

2 Thermal curing is an effective way to accelerate the curing of cementitious materials and can
3 be used for concreting in cold weather, in order to prevent frost damage. This study
4 investigates electric-thermal process curing of mortar at 20 °C and -10 °C. Fresh mortar
5 specimens were subjected to different electric potential differences and their internal and top
6 surface temperatures were monitored using a thermocouple and a thermal camera,
7 respectively. A theory for predicting the temperature increase of the mortar based on the
8 applied electric parameters was developed. Furthermore, the system was used to maintain the
9 internal temperature of mortar specimens at 10 °C for 12 hours while these were exposed to -
10 10 °C inside a cold room. Compressive and flexural strength results show that electric curing
11 can prevent frost damage. For example, 28 days compressive strength of normally cured
12 mortar specimens exposed to -10 °C was 27.2 MPa while mortar specimens subjected to
13 electric curing achieved a compressive strength of 51 MPa. Results from mercury intrusion
14 porosimetry tests showed an increase in porosity for normally cured specimens, which was
15 responsible for strength loss.

16 **Keywords**

17 Electric curing, Heat of hydration, Temperature distribution, Frost damage

18 **Abbreviations**

- 19 A Cross section area (m²)
20 c Specific heat capacity (J/kg °C)
21 h Heat transfer coefficient (W/m² °C)
22 I Current (A)
23 m Mass of the object (kg)
24 Q Energy (J)

1	Q_L	Energy loss (J)
2	ΔT	Temperature increase of the object under given energy ($^{\circ}\text{C}$)
3	T_f	Temperature at the end of heating ($^{\circ}\text{C}$)
4	T_i	Initial temperature ($^{\circ}\text{C}$)
5	R	Resistance (Ω)
6	V	Potential difference (V)
7	P	Power (W)
8	T	Time (s)

9

10 **Highlights**

- 11 • Electric curing parameters of mortar are derived.
- 12 • Electric curing of mortar prevents frost damage.
- 13 • Temperature increase of fresh mortar under EC can be accurately predicted.

14

15 **1 Introduction**

16 Cement based materials are the most used building materials worldwide. They are cheap and
 17 durable. However, the rate of strength development of cement based materials is slow and it
 18 takes them several days to become fully hardened. In addition, in cold weather the setting and
 19 hardening of concrete and mortar are delayed and there is a risk of frost damage potentially
 20 leading to weaker final products [1].

21 Accelerated curing of cement-based materials has been identified as an effective method to
 22 facilitate the development of their early age strength [1] . High early age strengths allow
 23 removing forms at an earlier age, accelerating the work schedule, reducing overall costs and,
 24 most importantly, making concreting possible in winter, where concreting is not permitted
 25 under normal conditions. There are several methods to accelerate the curing of cementitious
 26 materials, with steam curing being the most widely used method. However, steam curing is

1 only used in the precast industry due to the fact that large equipment such as a closed
2 chamber or vessel, a steam generator and conveyors, etc. are required. In addition, despite its
3 reliable and relatively easy controllable operation, steam curing has a very poor energy
4 efficiency. Furthermore, it also introduces a temperature gradient within the depth of the
5 specimens inducing internal stresses [2]. In the case of cold weather, in general, the
6 construction area is covered and heaters are used to keep the temperature of the structure
7 above freezing temperature. However, these methods are insufficient and practically difficult
8 to implement, therefore, often construction work is stopped until weather conditions are
9 acceptable for continuous concreting.

10 Electrical curing is another method of thermal curing which can be used to accelerate curing
11 of cementitious materials. Electrical curing is referred to as the passing of electricity directly
12 through cement based materials which, as a result of Joule Heating, causes the temperature of
13 the material to increase. The increase of temperature consequently accelerates the setting time
14 of the mortar [3] and higher early age compressive strength can be achieved.

15 When mortar is subjected to a potential difference, heat is generated through the mortar and
16 as a result its temperature increases. There are two curing methods commonly known as
17 direct and indirect mortar curing. In the direct curing the mortar is directly subjected to
18 potential difference through electrodes, whereas in the indirect curing method current is
19 passed through an embedded electrical resistance and as a result the resistance heats up
20 transferring the heat to the mortar by thermal conduction. Electrical energy which is
21 generated from the current flow through the embedded resistance is converted to thermal
22 energy through a process known as Joule Heating, which results in a temperature rise in the
23 mortar. Similarly to the conventional heating of cementitious material, indirect heating also
24 introduces a temperature gradient. On the other hand, the direct electric heating method
25 provides a uniform temperature across the depth of specimens.

1 The electrical conductivity of fresh mortar is due to the motion of ions in the water that is
2 contained in it. It has been shown that cement paste and mortar conductivity reaches its
3 maximum before the end of the final setting, after which the conductivity is reduced [3, 4].
4 As concrete hardening progresses, the conductivity of concrete decreases. In general, the
5 fully hardened conventional concrete has a very low conductivity, which depends on the
6 degree of its moisture content [5, 3]. This indicates that the electric curing of conventional
7 cementitious materials should be applied while they are in their fresh state in order for it to be
8 effective. As the conductivity of hardened cementitious materials is low (depending on the
9 degree of moisture), conductive admixtures or fillers are added to produce conductive mortar
10 and concrete [6]. The addition of conductive admixtures increases the conductivity of both
11 fresh and hardened mortar and concrete. The latter has been the subject of many researches
12 recently [7, 8, 9, 10]. In case of fresh mortar, some researchers [11, 12, 13] also suggested the
13 addition of carbon fibre, nano carbon fibre or graphene in order to increase the conductivity
14 of fresh cement based materials to facilitate electric curing and prevent frost damage. For
15 example, Liu et al. [14] reported addition of graphene to cement mortar in order to increase
16 conductivity and facilitate electric curing for specimens stored at freezer at -20 °C. Results
17 from Tian et al. [11] and Lie et al. [12] also show superior mechanical properties for electric
18 cured cement based materials with inclusion of carbon fibre at -20 °C. However, other
19 researchers reported the effectiveness of electric curing of concrete without addition of
20 conductive admixtures. For example, Wilson and Gupta [15] used direct electric curing to
21 increase temperature of concrete specimens to 80 °C and then maintained this temperature for
22 4 hours. Uygunoğlu and Hocaoglu [3] reported a decrease in final setting time for concrete
23 specimens by applying potential difference. Other researchers also reported using electric
24 curing method to accelerated early age strength of NaOH-activated fly ash based brick
25 mixture [16] and alkali activated fly ash concrete [17].

1 Electric curing of mortar can revolutionise the concreting in-situ by providing an efficient
2 heating method with lower initial capital investment in equipment and substantially lower
3 running costs in comparison to externally applied heating methods such as steam, autoclaving,
4 etc. The main requirement of electric curing is the availability of electric power, which is
5 normally available on site. Both alternate and direct currents have been used by researchers
6 for generating electric heating especially in hardened concrete for de-icing in bridges and
7 airports [18, 19].

8 This paper attempts to scientifically validate the effectiveness of electric curing of in situ and
9 precast mortar and it defines the relationship between electric curing and the properties of
10 fresh mortar. Relationships were derived between the key parameters of the mortar and the
11 electric input, to develop a prototype mobile electric curing system for onsite use which can
12 accelerate curing of mortar and make mortar use possible even in cold weather without any
13 addition of setting accelerators or antifreeze admixtures.

14 This research is part of an ongoing research to develop a conductive mortar for bricklaying in
15 winter where brickwork is not permitted under normal conditions. A conductive mortar has
16 been developed and field trials are currently in progress.

17 **2 Test programme**

18 Electric curing of cementitious materials is a potential technology to accelerate curing of
19 mortar and to enable concreting during winter. This paper develops a theory to predict
20 temperature increase of fresh mortar under an electrical potential difference. Laboratory
21 investigations were conducted to determine the parameters that influence the temperature rise
22 under electric curing such as electric current, potential difference, duration and properties of
23 the mortar including weight, specific heat and heat transfer coefficient. The laboratory

1 investigation involved subjecting fresh mortar specimens to a constant electrical potential
2 applied at 30 minutes after water was added to the mortar during mixing.

3 The top surface and internal temperature of specimens were monitored with a thermal camera
4 and thermocouples respectively. In addition, prism specimens were exposed to -10 °C for
5 first 12 hours after casting while their temperature was maintained at around 10 °C by
6 subjecting to 30 V AC current. The flexural and compressive strength were determined at 3, 7
7 and 28 days. Porosity of these specimens was also determined by means of mercury intrusion
8 porosimetry.

9 **2.1 Materials and equipment**

10 Mortar specimens were fabricated with Portland Cement CEM I 52.5 N conforming to the
11 European standard [20] and red sand (80% passing through 600 µm). The chemical
12 composition of the cement was determined by XRF (PANalytical MagiX Pro X-ray
13 Fluorescence) and is presented in Table 1. Mortar specimens were cast in polystyrene cube
14 moulds (50 mm, 75 mm, 100 mm and 150 mm cubes) and in prism moulds (40 × 40 × 160
15 mm³ and 75 × 75 × 300 mm³). The materials were mixed in a table mixer with different mix
16 proportions as shown in Table 2. One specimen for cubes and three specimens for 40 × 40 ×
17 160 mm³ prism were manufactured. Prism Mortar specimens were designed with cement sand
18 ratio of 1:3 and 1:6 (by weight) representing M12 and M6 mortar, respectively.

19 In the case of the mortars to be exposed to cold temperature (series III in Table 2), specimens
20 were fabricated with Portland Cement CEM I 52.5 N and coarse sharp sand (50% passing
21 through 600 µm). The cement sand ratio for these specimens was 1:2.

22 A 1125 VA CM22502 Single phase portable isolation transformer with 230 V input and 110
23 V output was used for the experiments. The actual output was 55±1 V due to the fact that the

1 output transformer is centre tap earthed. The output from the transformer was connected to a
 2 Variable Voltage Transformers (Multicomp Variac) with an output of 0 to 120% of the 110 V
 3 Transformer. The Potential difference and current were measured by a digital multimeter and
 4 a Trumeter LCD Digital Ammeter, respectively. Both voltage and AC current reported in this
 5 paper are referred to as RMS values.

6 In the case of DC current, this was generated from a TTi PL320QMD Digital bench power
 7 supply. Both voltage and current were adjusted and measured by means of the power supply.

8 Table 1: Chemical composition of Portland cement

Chemical component	SiO ₂	Al ₂ O ₃	Fe ₂ O ₃	CaO	MgO	K ₂ O	P ₂ O ₅	SO ₃	Other elements
CEM I (Mass %)	15.87	3.58	6.69	68.55	0.79	1.11	0.15	2.65	0.62

10 Table 2: Details of the mixes

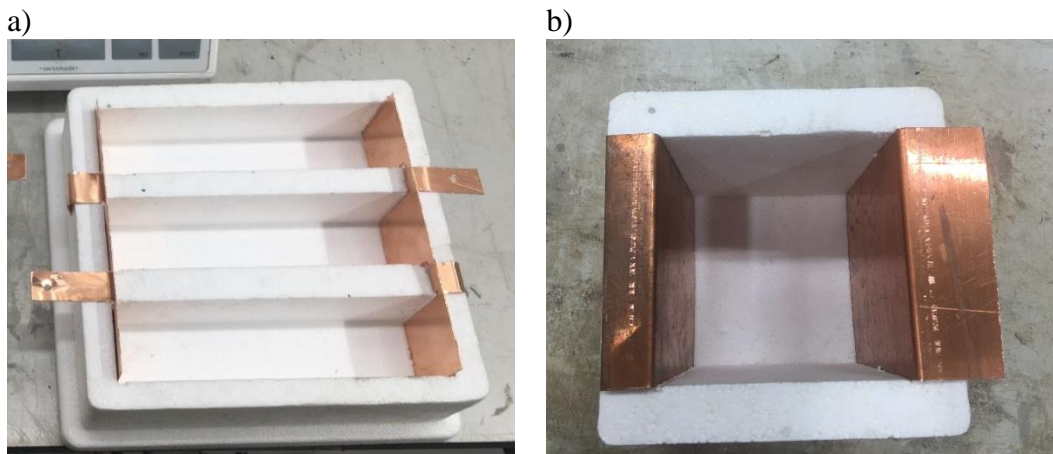
Series	Mix grade	Cement/Sand ratio	Water Cement ratio
Series I	M12	1:3	1.0
Series II	M6	1:6	2.0
Series III	M40	1:2	0.5

12 2.2 Details of the specimens, mixing and electric curing

13 2.2.1 Preparation of the moulds

14 As the standard steel moulds are not suitable for electric curing, polystyrene moulds were
 15 used throughout this research. Electrodes were placed at two opposite sides of the moulds and
 16 their shape and size were such to ensure full contact with the face of the cast mortar sample.
 17 Different electrode types have been used in other studies with hardened concrete especially
 18 for de-icing and snow melting purposes. These include copper [21], steel perforated, stainless
 19 steel [22], steel mesh and galvanised steel [21, 23], etc. However, all metallic materials are

1 identified as conductive and can be used as electrodes for mortar or conductive mortar as
2 mortar has an electrical resistivity much higher than any of these metals. The main
3 parameters to be considered are the surface area of the electrodes and the distance between
4 the electrodes connected to the concrete [24]. Electrodes for this study were obtained from a
5 copper sheet (thickness of 3 mm) and placed at two opposite faces of the mould as shown in
6 [Figure 1](#) for a three gang polystyrene mould ($40 \times 40 \times 160 \text{ mm}^3$) and 100 mm cube. The
7 electrodes are placed in such way that all three prisms are connected to the power in parallel.
8 The surface area of the copper sheet in contact to each prism face is $40 \times 40 \text{ mm}^2$. Similarly,
9 in the case of cube specimens, electrodes are located at two opposite sides of each cube
10 mould ([Figure 1b](#)).



11 [Figure 1](#): Preparation of the a) prism moulds and b) cubic mould prior to casting
12

13 **2.2.2 Mortar specimens for electric curing and surface temperature monitoring**

14 Specimens were cast in polystyrene cube moulds of 50, 75, 100 and 150 mm and polystyrene
15 prism moulds of $40 \times 40 \times 160 \text{ mm}^3$ and $75 \times 75 \times 300 \text{ mm}^3$. Details of the mixes are given
16 in [Table 3](#). Sand, cement and water were mixed together in a Hobart bench mixer for 3
17 minutes at low speed (140 RPM) in a laboratory environment (20 °C and 60% RH). At the
18 end of mixing, consistency of the mix was determined by the flow table test according to BS

1 EN 1015-3 [25]. Specimens were then cast in polystyrene moulds and compacted on a
 2 vibrating table. After 30 minutes from the addition of water to the mix, the specimens were
 3 subjected to potential differentials of 15, 30 or 60 Volts (Table 3). Temperature was
 4 measured at the centre of the top surface of each specimen at 0, 5, 10, 15, 20, 25 and 30
 5 minutes from the start of the application of the potential difference using a Flir i7 thermal
 6 camera. In the case of the three gang prism moulds, the temperature was measured at the
 7 centre of the top surface of the middle prism.

8 Internal temperatures of the specimens were also recorded during and after electric curing
 9 using thermocouples. A T type thermocouple was placed at the centroid of the cast mortar
 10 specimen (in the case of three gang prisms, at the centroid of the first prism). Temperature
 11 measurements were taken every 1-minute using a Data Taker DT 85G digital logger. The T
 12 type thermocouple is a fast response welded exposed junction with temperature range -76 °C
 13 to +250 °C.

14 Table 3: Details of the specimen sizes and potential differences for each series

Series	Mix No	Mix grade	Workability (mm)	Mould size (mm)	Potential difference (V)
Series I	1	M12	165	50	15
	2			50	30
	3			75	15
	4			75	30
	5			100	30
	6			100	60
	7			150	30
	8			40 × 40 × 160	30
	9			40 × 40 × 160	60
	10			75 × 75 × 300	30
	11			75 × 75 × 300	60
Series II	12	M6	158	40 × 40 × 160	60*
Series III	13	M40	198	40 × 40 × 160	30

15 * AC and DC current

1 **2.3 Testing**

2 **2.3.1 Flexural strength**

3 The flexural strength of the specimens was determined by a three point bending test. Three
4 prismatic specimens were used for each determination of flexural strength and the average
5 was calculated. Specimens were subjected to three point bending load on an Instron 3367
6 universal testing machine equipped with a 30 KN load cell, at room temperature. The load
7 was applied with a load rate of 30 N/s according to BS EN 1015-11:1999 [26]. Specimens
8 were tested at 3, 7 and 28 days to provide a flexural strength development profile.

9 **2.3.2 Compressive strength**

10 The compressive strength was determined on the two halves of the prisms obtained after the
11 three point bending test. Each half prism was subjected to compression loading using a test
12 frame model 7226/D/T/85248 CAP 3000 under load-control mode with a load rate of 400 N/s
13 according to BS EN 1015-11:1999 [26]. Two bearing plates ($40 \times 40 \times 10 \text{ mm}^3$) were placed
14 on the top and bottom of the half prism to create a surface area of $40 \times 40 \text{ mm}^2$. Therefore,
15 the compressive strength results presented here are referred to as equivalent compressive
16 strength. Specimens were tested at 3, 7 and 28 days to provide a compressive strength
17 development profile.

18 **2.3.3 Porosity and pore size distribution**

19 The porosity and pore size distribution were determined by Mercury Intrusion Porosimetry
20 (MIP) using a PASCAL 140/240 Porosimeter. MIP specimens were taken from the middle of
21 the specimens after the compression test at 28 days age. Each specimen weighed around 2 g.
22 Specimens were first dried in an oven at 105 °C for 3 days and then kept in a desiccator until
23 the MIP analysis was conducted. The porosity and pore size distribution were determined

1 using the mercury intrusion porosimetry technique. The pore size was calculated from the
2 pressure and volume data and computed by using the Washburn equation as follows:

$$3 \quad D = \frac{4\gamma\cos\theta}{P} \quad (1)$$

4 Where D is the diameter of the pores (nm); γ is the surface tension of the mercury ($\text{N}\cdot\text{m}^{-1}$);
5 θ is the contact angle between the mercury and the capillary pore surface (assumed as 140°)
6 and P is the applied pressure (Pa). The surface tension of mercury is $0.48 \text{ N}\cdot\text{m}^{-1}$.

7 **3 General relationship among electric curing parameters of mortar**

8 The energy required to increase the temperature of an object is determined by the general
9 thermodynamic relationships as follows:

$$10 \quad Q = mc\Delta T_h \quad (2)$$

$$11 \quad \Delta T_h = (T_f - T_i) \quad (3)$$

12 Where Q is the energy (Joule); m is the mass of the object to be heated (kg); c is the specific
13 heat capacity ($\text{J}/\text{kg}\cdot^\circ\text{C}$) which represent the amount of heat required to increase the
14 temperature of a unit mass by 1°C and it is determined experimentally by using a calorimeter
15 [27]. ΔT_h is the temperature increase of the object under a given energy. The temperature
16 increase ΔT_h is calculated from the initial temperature of the object or room temperature if
17 they are the same (T_i) and the temperature of the object at the end of the heating (T_f).

18 Equation 2 is based on the assumption of negligible heat loss, however, in practice there is
19 loss of heat to the environment, which can be determined using Newton's law of cooling as
20 follows:

$$21 \quad Q_L = Ah\Delta T_c \quad (4)$$

1
$$\Delta T_c = (T_f - T_r) \quad (5)$$

2 Where Q_L is the heat loss (*Joule*); A is the exposed surface area (m^2); h is a parameter that
3 measures the rate of energy transport towards the outside ($W/m^2 \cdot ^\circ C$); ΔT_c is the difference
4 between the temperature of the specimen at the end of heating T_f and the room temperature T_r .

5 Therefore, the total energy input to an object appears in the form of temperature increase and
6 heat loss to the environment that can be determined as follows:

7
$$Q = mc\Delta T_h + Ah\Delta T_c \quad (6)$$

8 [Equation 6](#) is a general thermodynamic equation used to calculate the temperature increase of
9 an object assuming that there is no phase change. When the initial temperature of the
10 specimen is similar to the room temperature, ΔT_h and ΔT_c can be equal.

11 The power produced by electricity can also be determined by the general electrical
12 relationships as follows:

13
$$P = IV = \frac{V^2}{R} = I^2R \quad (7)$$

14 Where P is the power (*Watt*); I is the current (*Ampere*); V is the potential difference (*Volt*)
15 and R is the resistance (Ω).

16 Power is energy per unit time, and if power is constant, the energy Q delivered in the time t is
17 given by the following equation:

18
$$Q = Pt \quad (8)$$

19 Where t is the time in seconds.

20 Substituting [Equation 7](#) into [Equation 8](#) gives the following expression for the electrical
21 energy:

1
$$Q=VIt \quad (9)$$

2 Therefore, the heat generated by passing current through an electrical resistance is directly
3 related to the voltage, current and the time that these parameters are applied.

4 Fresh mortar is conductive as it includes water. Subjecting fresh mortar to a potential
5 difference generates heat, which can be calculated from [Equations 6 and 9](#) as follows:

6
$$VIt = mc\Delta T_h + Ah\Delta T_c \quad (10)$$

7 Assuming $\Delta T_h = \Delta T_c = \Delta T$ when $T_i = T_r$, [Equation 10](#) can be used to calculate the
8 temperature increase in fresh mortar under a potential difference, as follows:

9
$$\Delta T = VIt \left(\frac{1}{mc + Ah} \right) \quad (11)$$

10
$$\Delta T = k \times t \quad (12)$$

11
$$k = \left(\frac{VI}{mc + Ah} \right) \quad (13)$$

12 [Equation 12](#) shows the relationship between temperature increase (°C) and the duration of
13 electric curing (second), potential difference (V), current (I) and k .

14 The critical parameters in [Equation 13](#) are the specific heat capacity (c) and the heat transfer
15 coefficient of fresh mortar and mould (h). These values can be measured experimentally. In
16 the case of metal, timber or polystyrene moulds, this value is generally constant for each
17 material and can be determined reasonably accurate. However, both heat transfer coefficient
18 and heat capacity of fresh mortar change with time as the hydration process causes the mortar
19 to set. Therefore, the values for c and h in [Equation 11](#) should be considered constant only
20 within a few hours from the start of mixing, before setting and heat development become
21 significant [\[20\]](#).

1 The mortar specimens for this study were cast in polystyrene moulds and their top surface
2 was covered during heating. Therefore, assuming that the heat loss is negligible, the above
3 equation can be rewritten as [Equation 14](#). However, this assumption is not valid when steel
4 mould is used or mortar specimen has a large exposed surface area.

$$5 \quad k = \left(\frac{VI}{mc}\right) \quad (14)$$

6 **4 Results and discussion**

7 **4.1 Temperature distribution**

8 **4.1.1 Comparison of AC and DC current**

9 In this study, fresh mortar specimens were cast in three gang prisms and subjected
10 continuously to a 60V constant potential difference for 30 minutes in both Alternate Current
11 (AC) and Direct Current (DC) and their top surface temperatures were monitored. The
12 potential difference was applied at 30 minutes after the addition of water to the mix. [Figure 2](#)
13 shows thermal images of the top surface of specimens subjected to both AC and DC at 0, 15
14 and 30 minutes of electric curing.

15 The mortar specimens in both three-gang polystyrene moulds ([Figure 2](#)) show similar top
16 surface datum temperatures of 21.6 °C (DC) and 21.4 °C (AC) before the application of the
17 constant potential difference (0 min). However, at the end of electric curing (30 min) the top
18 surface temperature reached 41.0 °C and 47.3 °C for DC and AC, respectively, indicating that
19 AC current produced 6.3 °C higher temperature compared to the DC current. These results
20 are in agreement with Galao et al. [\[19\]](#), who reported higher temperature increase for
21 hardened conductive mortar when subjected to 25 V AC compared to 25 V DC.

1 [Figure 2](#) also shows that AC current yields a uniform surface temperature distribution
2 whereas DC produces a non-uniform distribution across the top surface of the prisms. The
3 non- uniform temperature distribution is due to the polarisation effect which occurs when
4 water in the fresh mortar is subjected to DC current. The temperature difference increases
5 with increasing potential difference and water content in the mortar. The liberation of
6 hydrogen and oxygen gases was observed in mortar subjected to DC current due to
7 electrolyte conduction as shown in [Figure 3](#). [Figure 3](#) also shows chemical reactions
8 occurring between the mortar and the copper electrode at the anode under DC current. The
9 liberation of hydrogen and oxygen gases caused by chemical reactions was only observed in
10 mortar specimens subjected to DC current and the coating of rust (corrosion) was visible on
11 the electrodes after demoulding the samples. The rust coating also contributes to an increase
12 in the resistivity of the connection and hence, produces lower temperature of the mortar
13 compared to AC current. In addition, polarization due to the water also contributed to non
14 uniform temperature. Therefore, it was concluded that DC current is not suitable to cure fresh
15 mortar and hence the remaining investigations were carried out using AC current.

16

17

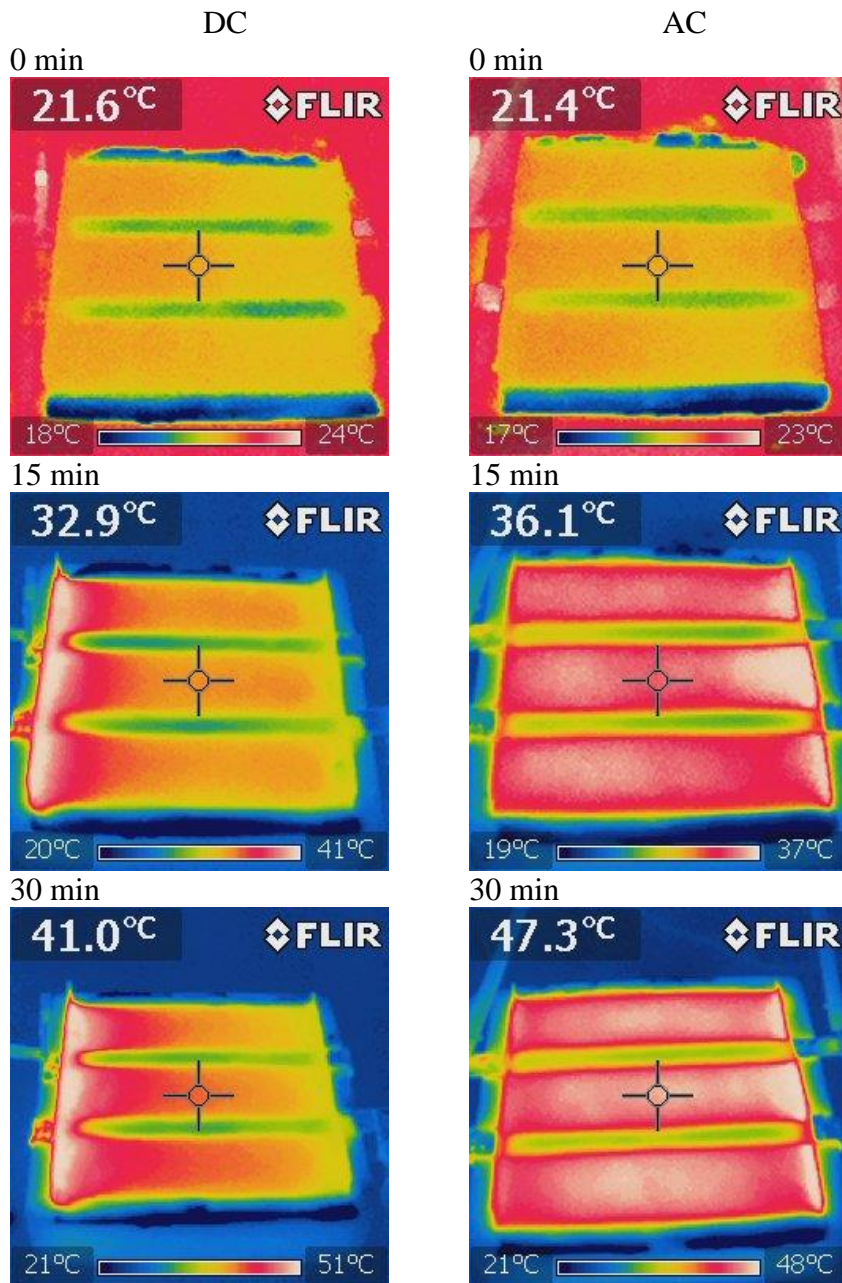
18

19

20

21

22



1 Figure 2: Top surface temperature of three gang prisms subjected to 60 Volts (a) DC and (b) AC
 2 current

3

4

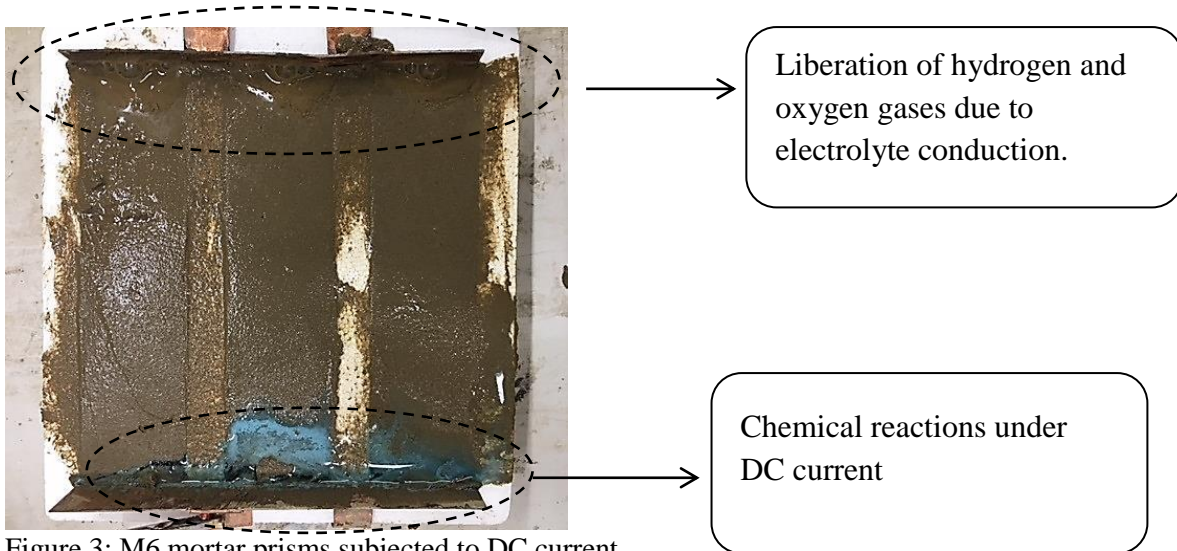


Figure 3: M6 mortar prisms subjected to DC current

1
2
3
4
5

4.1.2 Temperature increase under electric curing

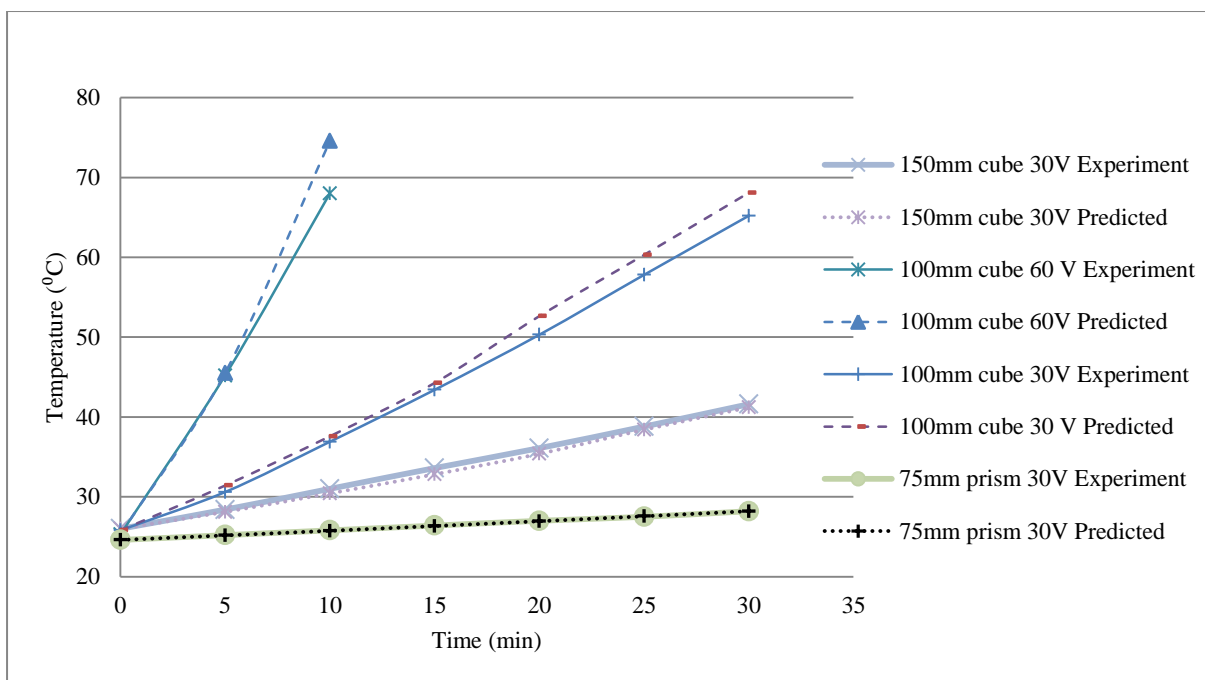
Mortar specimens were subjected to a constant potential difference and their top surface temperature was monitored. Table 4 summarises the results obtained in the tests and shows that increasing voltage increases the rate of the temperature rise. These results are in agreement with Uygunoğlu and Hoccoğlu [3], who reported a temperature increase for concrete specimens which were subjected to 40V, 60V and 100 V.

The temperatures of the specimens at the end of the electric curing ranged from 39 °C to 100 °C, while the temperature increase rate ranged from 0.5 °C/min to 2.6 °C/min. The rate of temperature increase is an important parameter in thermal curing as too rapid heating reduces the durability of the mortar.

The time-temperature relationship of the different mortar volumes at the voltages for mortar specimens were analysed to determine the rate of temperature increase with time, $\Delta T/t$ (slope k). k was predicted from Equation 12 and assumed that the heat loss was negligible since the

1 specimens were cast in polystyrene moulds and then covered with polystyrene lids during
 2 heating. Figure 4 shows the temperature-time relationships for some of the mortar specimens
 3 subjected to AC. A linear relationship was observed for k with all of the used mortar
 4 volume/voltages electric curing combinations. The continuous lines are based on the
 5 experimental investigation and the dashed lines are calculated from Equation 11. The
 6 calculated values are very close to the experimental data up to 45 °C, within a temperature
 7 difference of less than 1 °C. However, at higher temperatures, the difference between
 8 theoretical and experimental results is higher. For example, temperature predicted for 100
 9 mm cube specimen subjected to 60 V for 10 minutes, is 74.6 °C, whereas experimental
 10 results show a temperature of 68.0 °C (6.6 °C lower than predicted). This is due to the heat
 11 loss being more significant at the higher temperature differential with the ambient. However,
 12 in practice, the maximum temperature under electric curing should be limited to lower value
 13 of 40-45 °C [28] at which the heat loss can be ignored.

14



15

16

Figure 4: Temperature increase of mortar specimens with time at different voltage

1

2 Table 4: Summary of the test results

Mix No	Sample size (mm)	Duration of curing (min)	Voltage (V)	Initial temperature (°C)	Final temperature (°C)	Temperature increase (ΔT)
1	50	30	15	23.4	57.9	34.5
2	50	15	30	22.3	100	77.7
3	75	30	30	23.0	95.4	72.4
4	75	30	15	24.5	39.8	15.3
5	100	10	10	25.3	68.0	42.7
6	100	15	60	25.3	93.5	68.2
7	100	30	30	25.8	65.2	39.4
8	150	30	30	26.0	41.6	15.6

3

4 Data in [Table 4](#) show that the 100, 75 and 50 mm mortar cubes subjected to 60, 30 and 30
5 Volts, respectively, achieved a high temperature of nearly 100 °C at the end of the electric
6 curing. The mortar developed a series of cracks which were caused by rapid water
7 evaporation and shrinkage. [Figure 5](#) shows a typical 100 mm cube heated to about 90 °C
8 within 15 minutes of electric curing, which developed large cracks. The risks associated with
9 high temperature of mortar at early age on long term strength and durability is well known
10 [\[29\]](#). In order to avoid risk to durability caused by delayed ettringite formation, it is
11 important to keep the temperature of the mortar below 70 °C [\[30\]](#). A temperature of 40-45 °C
12 has been recommended previously by the authors [\[31\]](#) for microwave curing of repair
13 materials, which provides a similar uniform heating as electric curing.



1
2 Figure 5: 100 mm cube specimen heated to about 90 °C within 15 minutes. Electric curing started 30
3 minutes after water was added to the mix

4

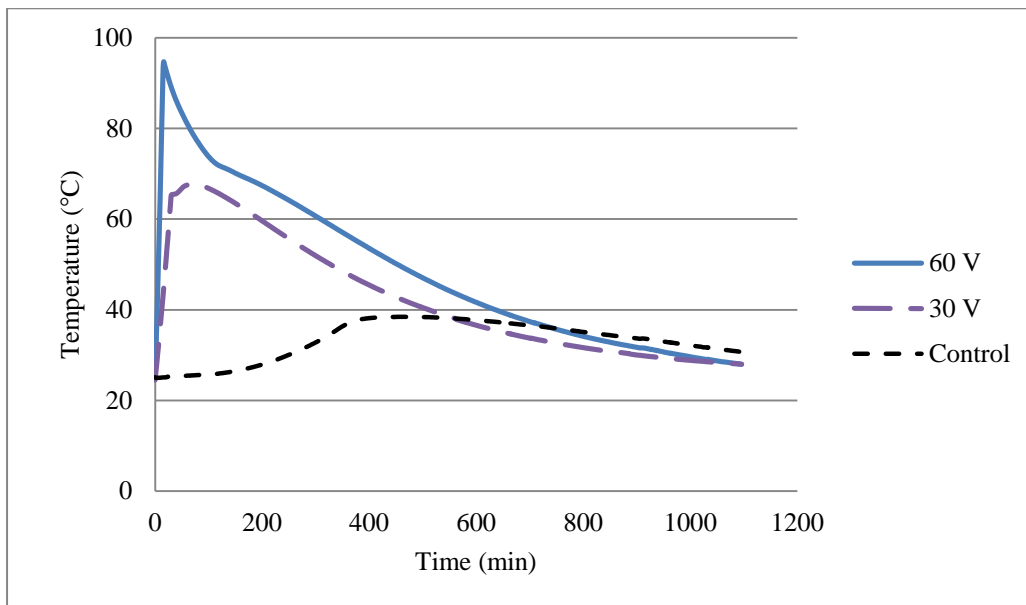
5 **4.2 Internal temperature development**

6 A T type thermocouple was located at the centre of cubic specimens or at the centre of one
7 prism in the case of three gang prism moulds. The temperature was monitored using a data
8 logger and recorded at one minute intervals for 24 hours after casting. [Figure 6](#) shows
9 temperature profiles of 100 mm cubes for a control specimen and specimens subjected to 30
10 V and 60 V. The tests were conducted in the laboratory at 22 °C ambient temperature. The
11 results show that the temperature of the control specimen started increasing at about 100
12 minutes from the start of the electric curing (130 minutes from the addition of water to the
13 mix) and it increased to about 37 °C at 350 minutes before gradually decreasing to room
14 temperature after about 1200 minutes. This temperature increase was due to the heat of
15 hydration, which is affected by several factors such as type of cement, cement content, mix
16 proportions, water/cement ratio, air temperature [\[28, 29\]](#). The temperature of the specimens

1 subjected to 30 V AC current reached 65 °C at the end of the 30 minutes electric curing and
2 then gradually decreased. Similar temperature decreases at the end of electric curing were
3 also recorded for all specimens subjected to potential differences.

4 The results presented here indicate that subjecting mortar to a potential difference increases
5 the temperature and makes the mortar reach its peak heat of hydration earlier compared to the
6 control specimens. This effect is also observed for other conventional heating methods [28,
7 32, 33], however, electric curing delivers a uniform temperature across the depth of the
8 mortar in a shorter time and hence there is no need for the long preheating period which is
9 required in steam curing.

10



11
12 Figure 6: Internal temperature of 100mm cube mortar (OPC cement sand ratio of 1:3) cured with 0, 30
13 and 60 Volts for a duration of 30 minutes

14

15 4.3 Temperature of mortar during freezing and thawing

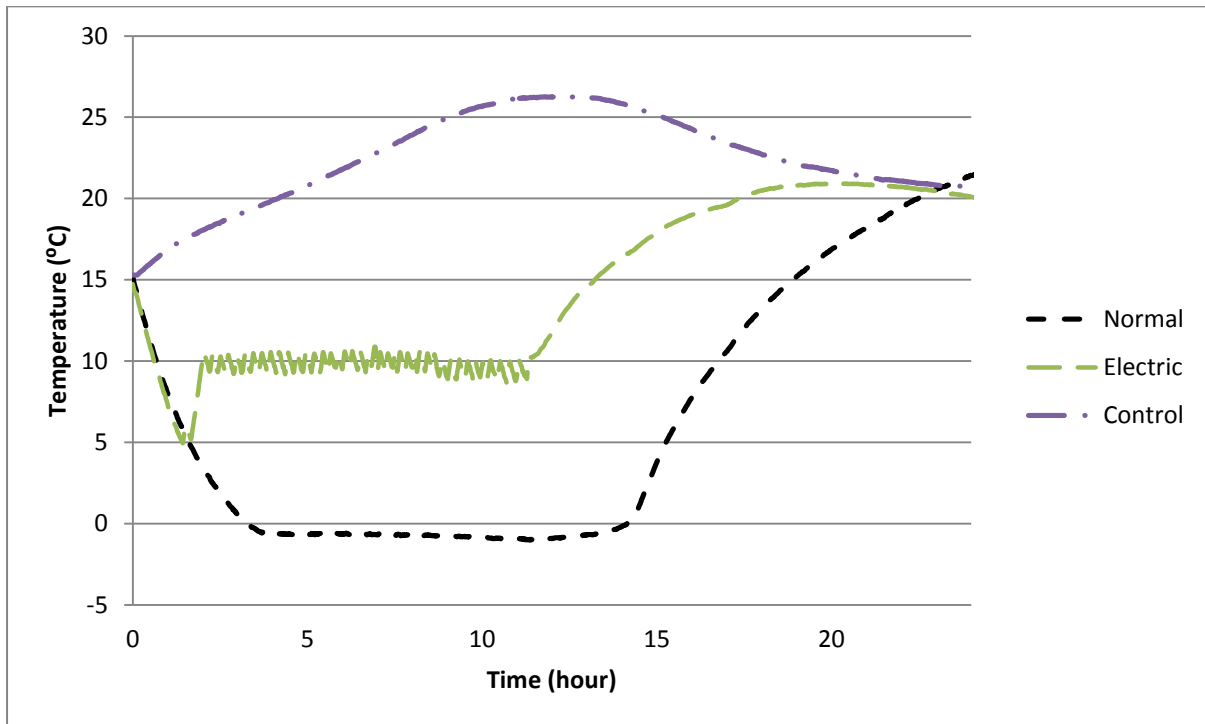
16 Concreting is not possible during cold weather due to the fact that fresh concrete is
17 vulnerable to frost damage. Electric curing has the potential to prevent frost damage of

1 mortar/concrete applied during cold weather. In this investigation, fresh mortar was exposed
2 to -10 °C for 12 hours to simulate freezing conditions during curing. A temperature controller
3 was used during electric curing to maintain the temperature of the mortar above 5 °C to
4 prevent frost damage. The internal temperatures of the specimens were monitored for 24
5 hours after casting by means of a T type thermocouple. [Figure 7](#) shows the recorded
6 temperature profiles. The control specimen was cast and cured at room temperature (18 °C
7 and 60% RH) for the whole period. The normal and electric curing specimens were cast at
8 room temperature and, at 30 minutes from the addition of water to the mix, these were
9 transferred to the cold room. Both control and electric curing specimens were exposed in the
10 cold room for 12 hours and then transferred to the laboratory (18 °C and 60 % RH). However,
11 electric curing specimens were subjected to 30 V AC while in the cold room to maintain the
12 internal temperature of the specimens at about 10 °C.

13 [Figure 7](#) shows that the temperature of the specimens not subjected to electric curing
14 (normal) gradually decreased from about 15 °C to about -0.5 °C before stabilising. Visual
15 observation confirmed the formation of ice on these specimens during the cooling period. A
16 temperature of 10 °C was selected to minimise the thermal stress caused by the temperature
17 of the cold room and Joule Heating.

18 One interesting observation from this temperature profile is that the internal temperature of
19 the normal specimens only reached -0.5 °C despite being exposed to -10 °C for 12 hours. A
20 similar behaviour was reported by Lee et al. [\[34\]](#) for concrete slab specimens (1200 × 600 ×
21 200 mm³) covered with 100 mm thickness of Styrofoam and exposed to -10 °C. In their case,
22 it took nearly 20 hours of exposure for the internal temperature of the specimens to reach
23 about -2 °C and almost 40 hours to achieve -10 °C. A more rapid temperature decrease was
24 observed by Yi et al. [\[35\]](#) for concrete specimens cast in steel moulds. This indicates that the

1 type of casting moulds has a significant effect on the internal temperature decrease of
2 concrete when this is exposed to cold weather.



3
4 Figure 7: Internal temperature of the mortar specimens

5

6 4.4 Flexural and compressive strength

7 [Table 5](#) presents the flexural strength with standard deviation of the prism specimens tested at
8 3, 7 and 28 days. Control specimens were cured entirely in the laboratory (18 °C and 60 %
9 RH). Each value is the average of three determinations. Electric cured and control specimens
10 showed similar flexural strength at 3, 7 and 28 days. However, the mortar specimens not
11 subjected to electric curing and exposed to -10 °C (normal) showed a significant reduction in
12 flexural strength, which can be attributed to frost damage. The reduction of flexural strength
13 is 122%, 31% and 35% at 3, 7 and 28 days age, respectively, for normal specimens compared
14 to the electric cured ones, indicating that the effect of frost damage is more severe at the early
15 age.

1 Data in Table 5 also presents the compressive strength results of specimens tested at 3, 7 and
 2 28 days age. Each value is the average of 6 measurements. The results illustrate that the
 3 compressive strength of normal specimens significantly suffered frost damage, with the
 4 compressive strength of electric cured specimens being almost 90% higher at 28 days. The
 5 compressive strength of the electric cured specimens is similar to that of the control
 6 specimens, showing that electric curing maintained the temperature of the specimens above
 7 freezing and prevented freezing of the fresh mortar. Data in Table 5 also show that the
 8 compressive strength decrease observed for the normal samples was similar for all of the
 9 testing ages.

10 A similar degree of reduction in compressive strength of concrete specimens was also
 11 reported by other researchers [35, 36] for exposures to -10 °C during 12 hours after casting.
 12 For example, Yi et al. [35] reported that the relative 28 day compressive strength of concrete
 13 specimens reduced by 50% when these were exposed to -10 °C for the first 12 hours after
 14 casting.

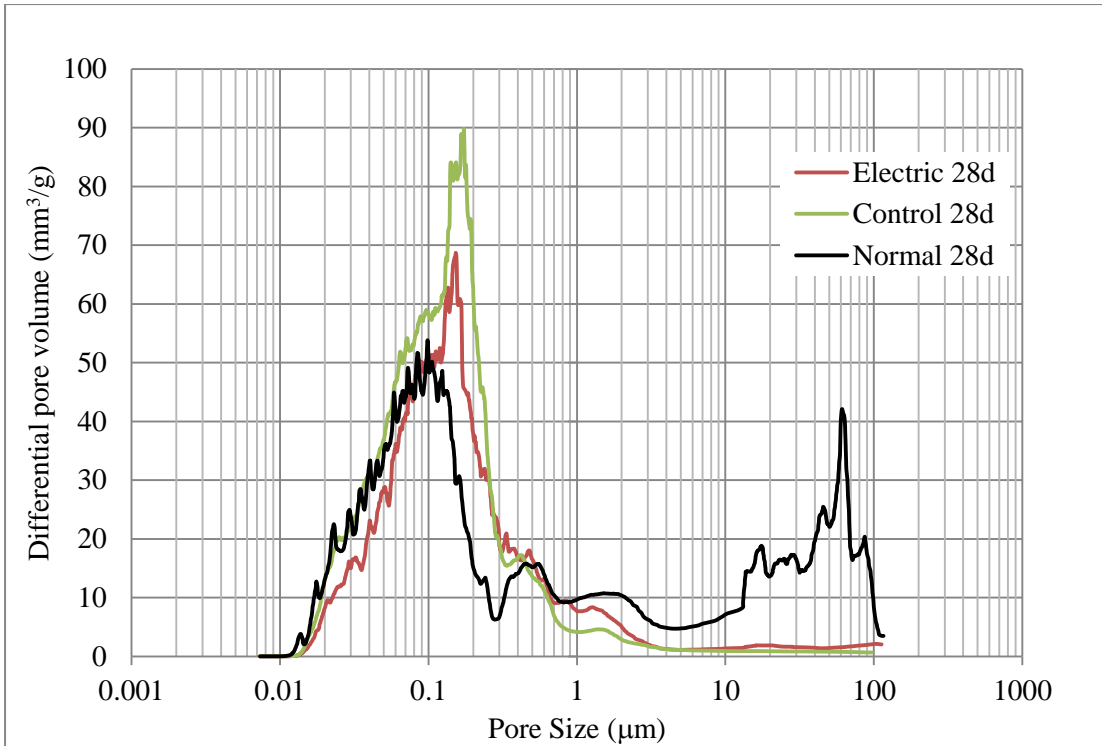
15 Table 5: Flexural strength, compressive strength and standard deviation of mortar specimens

Mix	Age (day)	Flexural strength (MPa)	Standard deviation (MPa)	Compressive strength (MPa)	Standard deviation (MPa)
Control	3	5.0	0.60	39.2	1.54
	7	5.5	0.44	48.5	3.90
	28	7.2	0.66	53.0	1.08
Normal	3	2.3	0.04	19.2	2.77
	7	3.9	0.26	26.3	3.54
	28	5.1	0.13	27.2	1.12
Electric	3	5.1	0.30	36.3	2.33
	7	5.4	0.26	50.9	3.31
	28	7.0	0.99	51.7	1.92

16

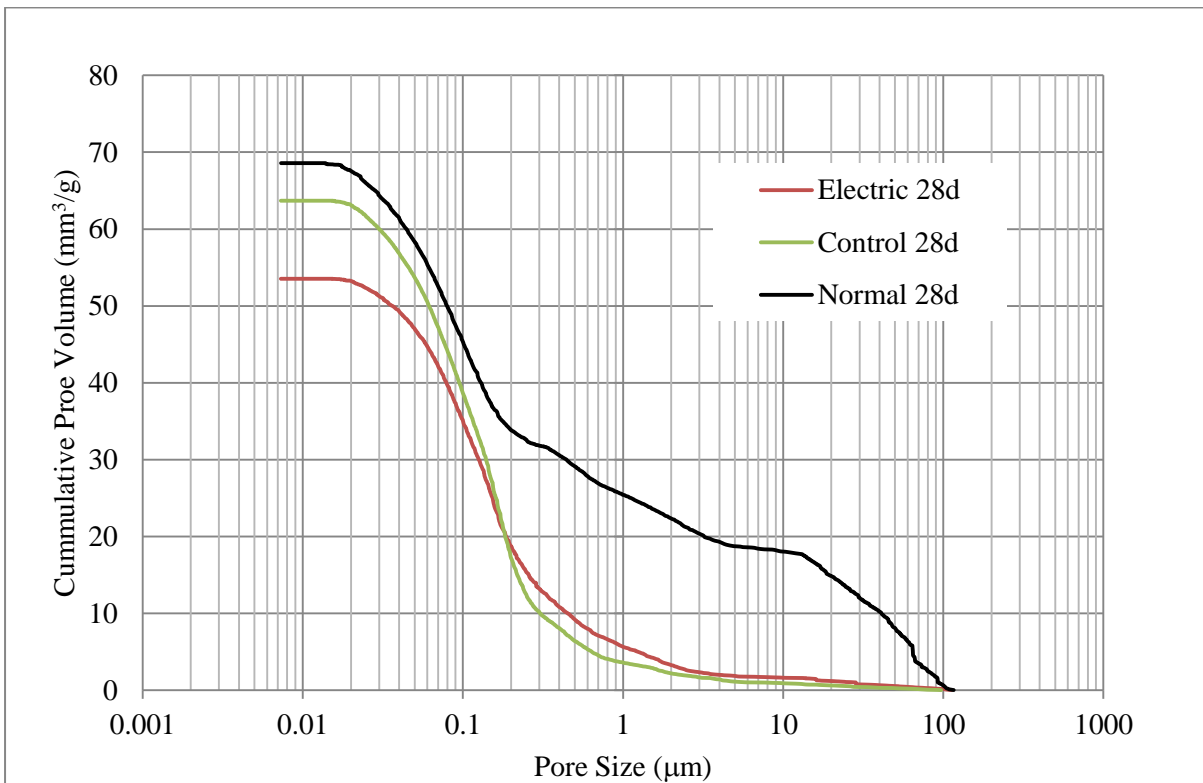
1 4.5 Porosity and pore structure

2 [Figure 8](#) shows the relationship between pore size and differential pore volume for the mortar
3 specimens at 28 days age. It shows the range of pore diameters under which significant levels
4 of differential pore volumes are observed. Control and electric cured specimens have a
5 unimodal pore distribution (range of 0.01-0.1 μm) which is typical for mortar specimens.
6 However, normal cured specimens show a double range of pore diameter (0.01-0.1 μm and
7 10-100 μm) with a significant differential pore volume that are separated by a diameter range
8 with smaller differential pore volume and categorised as a bimodal pore distribution [\[37\]](#).
9 This resulted in higher porosity for normally cured specimens and can be seen from [Figure 9](#).
10 Higher volume of porosity for the pore diameter larger than 10 μm indicates that damage was
11 caused due to exposure to frost conditions. This is in line with the results of the mechanical
12 strength tests. Fresh mortar (normally cured) subjected to freezing temperature produces
13 more pores with diameters larger than 10 μm . This is due to the fact that water present in
14 capillary and gel pores (smaller than 100 nm) does not freeze at temperatures around 0 $^{\circ}\text{C}$,
15 which is the internal temperature reported for the specimens (see [Section 4.3](#)).



1
2
3

Figure 8: Pore size distribution of the mortar specimens



4
5

Figure 9: Cumulative intruded volume of mortar specimens

1

2 **4.6 Practical application of the electric curing**

3 The advantages of introducing a method to increase the temperature of fresh mortar in a
4 controlled manner cannot be overstated. Such a method could be applied to accelerate the
5 curing of concrete to achieve rapid hardening of the mix in the construction of runways, roads
6 and precast industry without using accelerating admixtures. Furthermore, the controlled
7 heating of fresh mortars could allow their use at low temperatures, preventing the mortar
8 from being damaged by frost. Traditional methods such as steam curing or external heating
9 systems are either not practical on site or they are energy inefficient. Utilization of antifreeze
10 admixtures is also based on their category of minimum temperature at which they can be
11 effective. However, uncertainty about actual outdoor temperature during cold weather, makes
12 the selection of antifreeze admixtures difficult.

13 In this investigation, an electric curing method to increase the temperature of fresh cement
14 mortars was studied. The results indicated that there is a clear linear temperature increase
15 with time for specimens subjected to a constant potential difference. This means that the
16 temperature increase of the mortars can be accurately controlled. The factors to be considered
17 are power applied, mass and specific heat of the mortar [Equation 11]. This equation provides
18 an important input to the development of an automatic control algorithm for the operation of
19 a mortar electric curing system.

20 **5 Conclusions**

21 Applying an electric potential difference through a fresh mortar causes a temperature increase
22 of the material. The temperature at the end of the electric curing depends on the electric
23 power that is applied, which in turn depends on the size of the specimen and specific heat

1 capacity. The specimens subjected to electric curing showed a linear temperature increase
2 under a constant potential difference of up to nearly 100 °C.

3 Electric curing can be effectively used to prevent frost damage. This is shown by exposing
4 fresh mortar specimens to -10 °C during first 12 hours while a potential difference is used to
5 maintain specimen's temperature around 10 °C. Electric curing specimens show a flexural
6 and compressive strength of 6.9 and 50.9 MPa at 28 day respectively. The corresponding
7 strength for normal specimens exposed to -10 °C was 5.1 and 27.2 MPa for flexural and
8 compressive strength respectively.

9 Porosity of 28 day specimens determined by mercury porosimetry shows higher volume of
10 pores with diameters >10 µm for normal curing specimens exposed to -10 °C related to the
11 electric curing specimens. This shows that electric curing can prevent frost damage by
12 maintaining the temperature of the specimens above freezing temperature.

13 **Acknowledgements**

14 The authors gratefully acknowledge the funding provided by the Innovate UK and
15 Marlborough Brickwork Ltd for the "developing a conductive mortar for brickwork" project,
16 which produced this research, and a technology to cure brickwork is under development.

17 **Conflict of interest**

18 The authors declare that they have no conflict of interest.

19 **References**

- [1] Prerna Tighare, R. C. Singh, "Comparison of effect of hot water curing, steam curing & normal curing on strength of M20 grade of concrete," *International Journal for Research in Applied Science & Engineering Technology (IJRASET)*, vol. 5, no. 4, pp. 153-158, 2017.
- [2] Jinyan Shi, Baoju Liu, Feng Zhou, Shuai Shen, Jingdan Dai, Roujia Ji, Jinxia Tan, "Heat damage of concrete surfaces under steam curing and improvement measures,"

- Construction and Building Materials*, vol. 252, 2020, <https://doi.org/10.1016/j.conbuildmat.2020.119104>.
- [3] Tayfun Uygunoğlu, İsmail Hocoğlu, “Effect of electrical curing application on setting time of concrete with different stress intensity,” *Construction and Building Materials*, vol. 162, no. 20, pp. 298-305, 2018, doi.org/10.1016/j.conbuildmat.2017.12.036.
- [4] Xiaosheng Wei, Lianzhen Xiao, Zongjin Li, “Prediction of standard compressive strength of cement by the electrical resistivity measurement,” *Construction and Building Materials*, vol. 31, pp. 341-346, 2012, <https://doi.org/10.1016/j.conbuildmat.2011.12.111>.
- [5] K.R. Backe, O.B. Lile, S.K. Lyomov, “Characterizing curing cement slurries by electrical conductivity,” *Society of Petroleum Engineers*, vol. 16, no. 04, pp. 201-207, 2001.
- [6] Christopher Y. Tuan, Sherif A. Yehia, “Implementation of conductive concrete overlay for bridge deck deicing at Roca, Nebraska,” in *Sixth International Symposium on Snow Removal and Ice Control Technology*, Spokane, Washington, 2004.
- [7] Sherif Yehia, Christopher Y. Tuan, David Ferdon, and Bing Chen, “Conductive Concrete Overlay for Bridge Deck Deicing: Mixture Proportioning, Optimization, and Properties,” *American Concrete Institute*, vol. 97, no. 2, pp. 172-181, 2000.
- [8] Kasthurirangan Gopalakrishnan, Halil Ceylan, Sunghwan Kim, Shuo Yang, Hesham Abdulla, “Electrically Conductive mortar characterization for self-Heating airfield concrete pavement mix design,” *International Journal of Pavement Research and Technology*, vol. 8, no. 5, pp. 315-324, 2015.
- [9] Yehia Sherif, Host Joshua, “Conductive concrete for cathodic protection of bridge decks,” *ACI Materials Journal*, pp. 577-585, 2010.
- [10] Pooja Tambe, Sneha Paul, Akhil Sathbhai, Sc.Vala Krikiritkumar, Y. M. Ajar, “Conductive concrete shield for electronics against electro-magnetic pulse attack,” *Asian Journal of Convergence in Technology*, vol. IV, no. I, 2018.
- [11] Weichen Tian, Mingzhi Wang, Yushi Liu, Wei Wang, “Ohmic heating curing of high content fly ash blended cement-based composites towards sustainable green construction materials used in severe cold region,” *Journal of Cleaner Production*, vol. 276, pp. 1-11, 2020, <https://doi.org/10.1016/j.jclepro.2020.123300>.
- [12] Yushi Liu, Mingzhi Wang, Weichen Tian, Beimeng Qi, Zhongyao Lei, Wei Wang, “Ohmic heating curing of carbon fiber/carbon nanofiber synergistically strengthening cement-based composites as repair/reinforcement materials used in ultra-low temperature environment,” *Composites Part A: Applied Science and Manufacturing*, vol. 125, pp. 1-10, 2019, <https://doi.org/10.1016/j.compositesa.2019.105570>.
- [13] Weichen Tian, Beimeng Qi, Yushi Liu, Keqi Liu, Wei Wang, “Early frost resistance and permeability properties of carbon fiber/cement-based composite cured by ohmic heating under ultra-low temperature,” *Construction and Building Materials*, vol. 282, pp. 1-14, 2021, <https://doi.org/10.1016/j.conbuildmat.2021.122729>.
- [14] Yushi Liu, Mingzhi Wang, Wei Wang, “Electric induced curing of graphene/cement-based composites for structural strength formation in deep-freeze low temperature,” *Materials & Design*, vol. 160, pp. 783-793, 2018, <https://doi.org/10.1016/j.matdes.2018.10.008>.
- [15] John Gibb Wilson, Narendra Kumar Gupta, “Equipment for the investigation of the accelerated curing of concrete using direct electrical conduction,” *Measurement*, vol. 35, no. 3, pp. 243-250, 2004, <https://doi.org/10.1016/j.measurement.2003.11.002>.

- [16] Mateusz Ziolkowski, Maxim Kovtun, “Confined-Direct Electric Curing of NaOH-activated fly ash based brick mixtures under free drainage conditions: Part 2. Confined-DEC versus oven curing,” *Construction and Building Materials*, Vols. 176, <https://doi.org/10.1016/j.conbuildmat.2018.05.041>, pp. 452-461, 2018.
- [17] Maxim Kovtun, Mateusz Ziolkowski, Julia Shekhovtsova, Elsabe Kearsley, “Direct electric curing of alkali-activated fly ash concretes: a tool for wider utilization of fly ashes,” *Journal of Cleaner Production*, vol. 133, pp. 220-227, 2016, <http://dx.doi.org/10.1016/j.jclepro.2016.05.098>.
- [18] J.Gomis, O.Galao, V.Gomisb, E.Zornoza, P.Garcés, “Self-heating and deicing conductive cement. Experimental study and modeling,” *Construction and Building Materials*, vol. 75, pp. 442-449, 2015, <https://doi.org/10.1016/j.conbuildmat.2014.11.042>.
- [19] Oscar Galao, , Luis Bañón, , Francisco Javier Baeza, Jesús Carmona, Pedro Garcés, “Highly conductive carbon fiber reinforced concrete for icing prevention and curing,” *Materials*, vol. 9, no. 4, pp. 1-14, 2016, <https://doi.org/10.3390/ma9040281>.
- [20] “BS EN 197-1: Cement- Part 1: Composition, specification and conformity criteria for common cements,” 2011.
- [21] Ruohong Zhao, Christopher Y. Tuan, Daobo Fan, An Xu, and Bao Luo, “Ionically conductive mortar for electrical heating,” *ACI Materials Journal*, vol. 114, no. 6, pp. 923-933, 2017.
- [22] P. J. Tumidajski, “Electrical conductivity of Portland cement mortars,” *Cement and Concrete Research*, vol. 26, no. 4, pp. 529-534, 1996.
- [23] Hesham Abdualla, Halil Ceylan, Sunghwan Kim, Mani Mina, Kasthurirangan Gopalakrishnan, Alireza Sassani, Peter C. Taylor, Kristen S. Cetin, “Configuration of electrodes for electrically conductive concrete heated pavement systems,” in *International Conference on Highway Pavements and Airfield Technology 2017*, Philadelphia, Pennsylvania, 2017.
- [24] J. M. Gandía-Romero, J. E. Ramón, R. Bataller, D. G. Palací, M. Valcuende, J. Soto, “Influence of the area and distance between electrodes on resistivity measurements of concrete,” *Materials and Structures*, vol. 50, no. 17, 2017, <https://doi.org/10.1617/s11527-016-0925-2>.
- [25] “BS EN 1015-3 Methods of test for mortar for masonry- Part 3: Determination of consistence of fresh mortar (by flow table),” 1999.
- [26] “BS EN 1015-11:1999 Methods of test for mortar for masonry. Determination of flexural and compressive strength of hardened mortar,” 1999.
- [27] “ASTM E1269-2018 Standard test method for determining specific heat capacity by differential scanning calorimetry,” 2018.
- [28] P. S. Mangat, S. Abubakri, K. Grigoriadis, V. Starinieri, “Hydration and microwave curing temperature interactions of repair mortars,” *Recent Progress in Materials*, vol. 3, no. 4, 2021.
- [29] A. M. Neville, *Properties of Concrete*, Essex: Pearson Education Limited, 2011.
- [30] Steven H. Kosmatka, Beatrix Kerkhoff, and William C. Panarese, *Design and Control of Concrete Mixtures*, Portland Cement Association, 2003.
- [31] P.S. Mangat, K. Grigoriadis, S. Abubakri, “Microwave curing parameters of in-situ concrete repairs,” *Construction and Building Materials*, vol. 112, pp. 856-866, 2016, <https://doi.org/10.1016/j.conbuildmat.2016.03.007>.

- [32] J Ivan Escalante-Garcia, J. H. Sharp, “The effect of temperature on the early hydration of portland cement and blended cements,” *Advances in Cement Research*, vol. 12, no. 3, pp. 121-130, 2000, doi.org/10.1680/adcr.2000.12.3.121.
- [33] J. Hill, B.R. Whittle, J.H. Sharp, M. Hayes, “Effect of elevated curing temperature on early hydration and microstructure of composites,” in *Proceedings of the Materials Research Society Symposium*, 2003.
- [34] G.C. Lee, M.C. Han, D.H. Baek, K.T. Koh, “Effect of heat curing methods on the temperature history and strength development of slab concrete for nuclear power plant structures in cold climates,” *Nuclear Engineering and Technology*, vol. 44, no. 5, pp. 523-534, 2012, https://doi.org/10.5516/NET.09.2011.074.
- [35] Seong-Tae Yi, Sue-Won Pae, Jin-Keun Kim, “Minimum curing time prediction of early-age concrete to prevent frost damage,” *Construction and Building Materials*, vol. 25, pp. 1439-1449, 2011, https://doi.org/10.1016/j.conbuildmat.2010.09.021.
- [36] Jin-Keun Kim, In-Yeop Chu, Seong-Tae Yi, “Minimum curing time for preventing frost damage of early-age concrete,” *The IES Journal Part A: Civil & Structural Engineering*, vol. 1, no. 3, pp. 209-217, 2008.
- [37] P.S. Mangat, Olalekan O. Ojedokun, “Influence of curing on pore properties and strength of alkali activated,” *Construction and Building Materials*, vol. 188, pp. 337-348, 2016, https://doi.org/10.1016/j.conbuildmat.2018.07.180.

1

2